Available online at www.sciencedirect.com
ScienceDirect
Catalysis Today 129 (2007) 305–312
CATALYSIS TODAY
www.elsevier.com/locate/cattod

Steam reforming of ethanol over Co_3O_4/CeO_2 catalysts prepared by different methods

H. Wang, J.L. Ye, Y. Liu *, Y.D. Li, Y.N. Qin

Department of Catalysis Sciences and Technology, School of Chemical Engineering, Tianjin University, Tianjin 300072, China

Available online 27 September 2007

Abstract

In this paper, Co_3O_4/CeO_2 catalysts for steam reforming of ethanol (SRE) were prepared by co-precipitation and impregnation methods. The catalysts prepared by co-precipitation were very active and selective for SRE. Over 10%Co_3O_4/CeO_2 catalyst, ethanol conversion was close to 100% and hydrogen selectivity was about 70% at 450 °C. The catalysts were characterized by X-ray diffraction, temperature-programmed reduction (TPR) and BET surface area measurements. The preparation method influenced the interaction between cobalt and CeO_2 evidently. The incorporation of Co ions into CeO_2 crystal lattice resulted in weaker interaction between cobalt and ceria on catalyst surface. In comparison with catalysts prepared by impregnation, more cobalt ions entered into CeO_2 lattice, and resulted in weaker interaction between active phase and ceria on surface of Co_3O_4/CeO_2 prepared by co-precipitation. Thus, cobalt oxides was easier to be reduced to metal cobalt which was the key active component for SRE. Meanwhile, the incorporation of Co ions into CeO_2 crystal lattice was beneficial for resistance to carbon deposition.

Keywords: Ethanol; Steam reforming; Ceria; Cobalt; Hydrogen; Mixed oxide; Fuel cell

1. Introduction

Fuel cells have recently attracted much attention for the application to power vehicles or small stationary power units [1]. The primary hydrogen production routes include reforming or partial oxidation of hydrocarbons and alcohols [2–4]. Steam reforming of ethanol (SRE) is an attractive option as ethanol is less toxic than methanol and can be produced from biomass without net addition of carbon dioxide to the atmosphere [5–7].

The catalysts so far used for the process can be classified into three categories: oxide catalysts, noble metal catalysts and base metal catalysts. Oxide catalysts, such as MgO, Al_2O_3, V_2O_5, ZnO, TiO_2, La_2O_3, CeO_2, Sm_2O_3, La_2O_3-Al_2O_3, CeO_2-Al_2O_3, MgO-Al_2O_3. Al_2O_3 and V_2O_5 catalysts, show good activity but insufficient selectivity [8,9]. ZnO exhibits high activity and good selectivity for SRE, however, its stability has not been reported. Noble metal catalysts, such as Rh, Pt and Pd, are active for SRE, but the amount of loading of noble metal is high, generally close to 5%, thus the cost is high [10–15]. The base metal catalysts reported include Co-based, Cu-based and Ni-based catalysts [16–19]. Ni/Al_2O_3 gives a high ethanol conversion and the H_2 selectivity reaches to 70% at 500 °C. But the acidity of Al_2O_3 results in coke deposition and a severe deactivation [20]. In addition, for the Ni-based catalysts, CH_4 or CO content in the products is comparatively high. Cu-based catalysts exhibit good activity at low reaction temperature, while H_2 selectivity is poor [21,22]. The Co-based catalysts exhibit good activity and products distribution [23–25]. Among the Co-based catalysts reported, Co/ZnO shows the best catalytic performance [26–28]. However, they may rapidly deactivate during on-stream operation due to coke formation, cobalt oxidation or sintering [29].

The support plays an important role in catalyst stability [30]. CeO_2 has an oxygen storage property because of high oxygen mobility in its lattice. Therefore, ceria-based catalysts may be a good choice for elevating resistance to coke formation [31]. CeO_2 is inclined to interact with some metal active component which effect on redox behavior of metal component and lead to high dispersion of active component. Velu and co-workers [32,33] presented that Ni-Rh bimetallic catalysts supported on CeO_2 exhibited very good catalytic performance for SRE.

Several works examined Co/CeO_2 catalysts for Fischer–Tropsch reaction and carbon monoxide oxidation [34,35]. Llorca et al. [26–28] investigated Co catalysts prepared by

* Corresponding author.
E-mail address: yuanliu@tju.edu.cn (Y. Liu).

0920-5861/$ – see front matter © 2007 Elsevier B.V. All rights reserved.
doi:10.1016/j.cattod.2006.10.012

impregnation method using $Co_2(CO)_8$ as the precursor and supported on several oxides.

In this work, Co_3O_4/CeO_2 catalysts were prepared by co-precipitation and impregnation, respectively, and it was found that the co-precipitated catalyst exhibits better catalytic activity and selectivity for SRE. The structure and catalytic performance of the catalyst were investigated and discussed.

2. Experimental

2.1. Catalyst preparation

2.1.1. Co-precipitation

The solution of cobalt nitrate (0.5 mol/l) and the solution of cerium nitrate (0.5 mol/l) were mixed at certain molar ratios and used as metal precursors, which was named as solution A. The sodium carbonate solution, referred to as solution B, was used as a precipitator. Solutions of A and B were merged into distilled water with a pH 7.5–8.5, and continued stirring for 4 h. The resulting precipitate was aged at room temperature for 24 h and then was filtrated and washed with de-ionized water for several times. The precipitate was dried at 80 °C for 12 h and calcined at 650 °C for 2 h. The catalyst obtained in this method was referred to as $x Co_3O_4/CeO_2$-C, where x stands for Co content in weight and C represents co-precipitation.

2.1.2. Impregnation

CeO_2 support was prepared by precipitation. Co_3O_4/CeO_2 catalysts were prepared by impregnation method using an aqueous solution of cobalt nitrate. Then, the deposits were dried for 24 h at room temperature and at 80 °C for 12 h. The samples were finally calcined at 650 °C for 2 h. The catalyst obtained in this method was denoted as $10\%Co_3O_4/CeO_2$-I, where I stands for sample prepared by impregnation.

2.2. Catalytic performance tests

Catalytic performance tests were performed in a fixed-bed quartz reactor at atmospheric pressure. About 150 mg catalysts with 40–60 mesh grain size were loaded into the reactor. Prior to each reaction, the system was outgased with N_2 for 10 min, then reduced in H_2/Ar at 650 °C for 40 min and then cooled down to 350 °C.

A premixed water–ethanol solution with a water to ethanol molar ratio of 3:1 was fed into the reactor through a pump. The feed was preheated at 140 °C, vaporized and mixed with 80 vol% N_2. The space velocity was 40,000 ml g_{cat}^{-1} h^{-1} (that is 1,00,000 h^{-1}) and reaction temperature was from 350 to 600 °C. The effluent gases were analyzed online by two gas chromatographs with two columns. The effluent of the reactor was heated before entering into the GC. Porapack Q packed column was used to analyze N_2, water, acetaldehyde, ethanol and acetone. H_2, N_2, CO, CH_4 and CO_2 were separated by TDX-01 column. Nitrogen was used as an internal standard to calculate the carbon and hydrogen balance.

As a result of the products variation, the catalyst performance was characterized by two parameters. S_i represents the product distribution of i; Y_{H_2} expresses the mol yield of hydrogen. Ethanol conversion denoted as X_{EtOH}. They were calculated according to Eqs. (1)–(3):

$$X_{EtOH} = \frac{\text{mol EtOH}_{in} - \text{mol EtOH}_{out}}{\text{mol EtOH}_{in}} 100\% \quad (1)$$

$$S_i = \frac{\text{mol } P_i}{\sum_{i=1}^{n} \text{mol } P_i} 100\% \quad (2)$$

$$Y_{H_2} = \frac{\text{mol H}_2}{\text{mol EtOH}_{in} - \text{mol EtOH}_{out}} \quad (3)$$

where P_i is the molar amount of each product.

2.3. Catalyst characterization

The BET surface areas of catalysts were measured by nitrogen adsorption at liquid nitrogen temperature using a Micromeritics ASAP 2010 analyzer. X-ray diffraction (XRD) analysis was performed on a Philip X'pert Pro instrument. Co Kα radiation was used with 40 kV and 100 mA. In situ XRD was performed with Philip X'pert Pro diffractometer using Co Kα radiation. The sample was supported on a disk of 2 cm in diameter. The 5 vol% H_2/Ar gas was passed through the catalyst bed at a flow rate of 30 ml/min. The temperature of the catalyst was measured by a thermocouple situated inside the catalyst layer. The heating rate was 10 °C/min. The temperature was raised from 350 to 800 °C, and in situ XRD data were collected at each interval of 50 °C. At 350, 650 and 800 °C, the temperature was retained for 40 min, and at other temperature points for 10 min, respectively.

TPR of catalysts in a $5\%H_2/N_2$ (20 ml/min) gas mixture was carried out in a Thermo-Finnigan instrument. About 30 mg of the catalyst was loaded in a quartz tube reactor. The catalyst was heated in the gas mixture from room temperature to 900 °C with a heating rate of 10 °C/min and then kept for 10 min. The TG-DTA experiments were performed between ambient and 1000 °C with a heating rate of 10 °C/min and in flowing air. 4.0–6.0 mg catalysts were used.

3. Results

3.1. Catalytic performance tests

3.1.1. The effect of cobalt content on catalyst performance

Figs. 1 and 2 showed ethanol conversion and H_2 yield at selected temperature with cobalt contents ranging from 1 to 30 wt%. When reaction temperature was lower than 450 °C, the conversion of ethanol over Co_3O_4/CeO_2 increased with increase of cobalt content up to a Co_3O_4 content of 10 wt%, and then decreased with further increasing of the Co_3O_4 content over 10 wt%. At 500 °C or higher temperatures, all catalysts showed nearly 100% conversion except $1\%Co_3O_4/CeO_2$-C. The catalyst containing $10\%Co_3O_4$ was the most active among the samples tested. The H_2 yield was nearly similar over different catalysts except a little lower over $1\%Co_3O_4/CeO_2$-C.

Fig. 3 showed product distribution of SRE over 10%Co/CeO_2-C catalyst from 350 to 600 °C. Products mainly

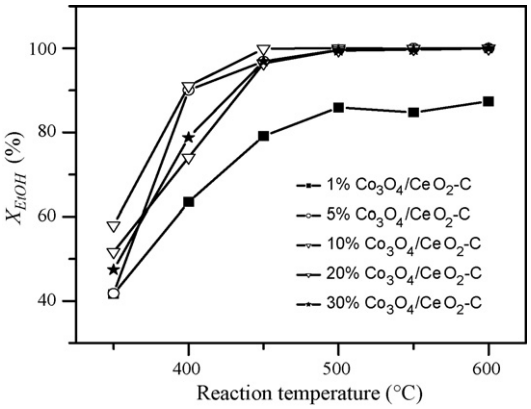

Fig. 1. C_2H_5OH conversion vs. reaction temperature over Co_3O_4/CeO_2 catalysts.

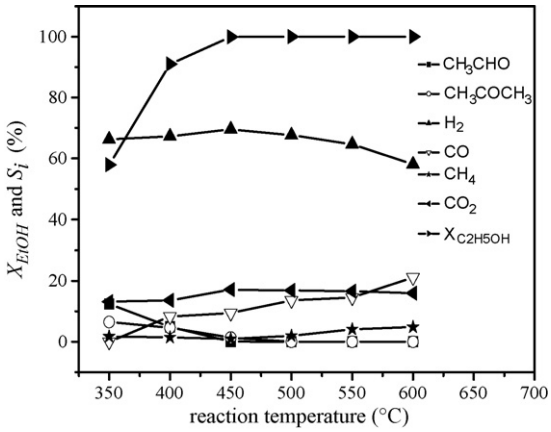

Fig. 3. Conversion of ethanol and product distribution vs. reaction temperature over 10%Co_3O_4/CeO_2-C catalyst.

contained H_2, CH_4, CO and CO_2. At low temperature (350 and 450 °C) there existed some acetaldehyde and acetone. With the increase of temperature, acetaldehyde and acetone converted to C1 products. Besides, it was obvious that CH_4 was kept at low level at all temperature range, which was lower than 5%. H_2 selectivity decreased accompanying with increase of CO selectivity with temperature increases, when temperature was higher than 450 °C.

In summary, the 10%Co_3O_4/CeO_2-C catalyst showed the best performance among the catalysts tested, exhibiting a high ethanol conversion and hydrogen yield. At 450 °C, ethanol conversion is nearly close to 100% and H_2 yield reaches 2.9 mol/mol C_2H_5OH.

3.1.2. The effect of preparation method on catalyst performance

Fig. 4 and Table 1 showed catalytic performance over 10%Co_3O_4/CeO_2 catalysts with different preparation methods. The preparation method affected on catalyst activity significantly. Ethanol conversion was close to 100% over 10%Co_3O_4/CeO_2-C while it was about 83% over 10%Co_3O_4/CeO_2-I at 450 °C. So it is obvious that catalyst prepared by co-precipitation is more active for SRE.

According to products distribution over the catalysts with different preparation methods listed in Table 1, catalyst prepared by co-precipitation method showed better product distribution than that obtained on catalysts prepared by impregnation. Its selectivity towards C2 (acetaldehyde, acetone) was lower, meanwhile, H_2 yield was high over catalyst prepared by co-precipitation, indicating that catalyst prepared by co-precipitation method is more favorable for SRE.

Ethanol conversion and products distribution were listed in Table 2 over the catalysts prepared by different methods at a higher space velocity of 1,20,000 ml h^{-1} $g_{cat}{}^{-1}$. The results revealed that 10%Co_3O_4/CeO_2-C showed high ethanol conversion even under high velocity of 1,20,000 ml h^{-1} $g_{cat}{}^{-1}$. At 450 °C, ethanol conversion was 82.1%. From 350 to 450 °C, H_2 selectivity was about 69%. On the other side over 10%Co_3O_4/CeO_2-I catalyst, ethanol conversion was lower than 20% at all the tested temperatures of Table 2. As for product distribution, the content of acetone was higher than 15%. The results indicated that 10%Co_3O_4/CeO_2-C catalyst was much more active than 10%Co_3O_4/CeO_2-I catalyst.

It has been reported that Co/CeO_2 catalyst was prepared by impregnation with $Co_2(CO)_8$ as precursor [28]. For this

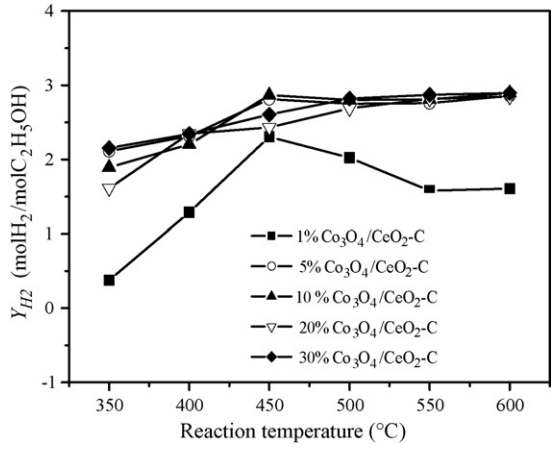

Fig. 2. H_2 yield vs. reaction temperature over Co_3O_4/CeO_2 catalysts.

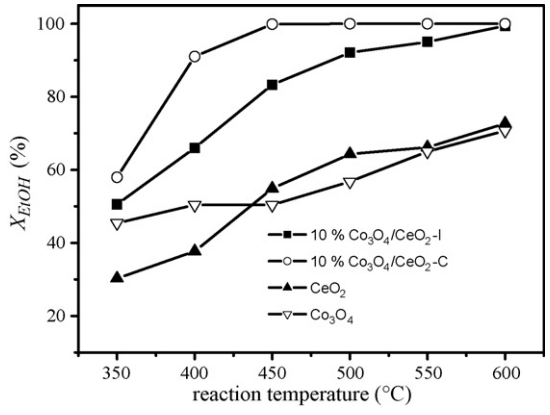

Fig. 4. C_2H_5OH conversion vs. reaction temperature over Co_3O_4, CeO_2 and Co_3O_4/CeO_2 catalysts.

Table 1
Product distribution and H_2 yield over Co_3O_4, CeO_2 and Co_3O_4/CeO_2 catalysts

Catalysts	Reaction temperature (°C)	Product distribution S_i (%)							Y_{H_2} (mol/mol)
		H_2	C_2H_4	CO	CO_2	CH_4	CH_3CHO	CH_3COCH_3	
10%Co_3O_4/CeO_2-I	450	66.7	0	5.6	16.3	0.2	5.1	6.1	2.4
10%Co_3O_4/CeO_2-C	450	69.9	0	8.9	18.8	0.9	0.1	1.3	2.9
Co_3O_4	450	65.8	11.1	7.1	0	0	15.9	0	0.8
CeO_2	450	55.5	21.0	0	8.2	0	4.3	10.9	0.3
10%Co_3O_4/CeO_2-I	500	63.9	0	9.2	17.9	0.9	3.0	5.1	2.7
10%Co_3O_4/CeO_2-C	500	67.7	0	13.6	16.8	1.9	0	0	2.8
Co_3O_4	500	64.1	7.9	7.5	6.0	1.1	13.4	0	1.3
CeO_2	500	65.8	6.6	5.4	13.1	0	1.8	7.3	0.9

catalyst, ethanol conversion and H_2 selectivity was to 93.7 and 69.6%, respectively, at 450 °C and under space velocity of 5000 h^{-1} and water/ethanol 13, while the coke deposition was severe. In this work, Co_3O_4/CeO_2 catalysts showed higher activity and comparable H_2 selectivity under more rigorous conditions, suggesting that the preparation method markedly affect catalytic performance. For SRE reaction over other composite catalysts, preparation method also influenced catalytic performance evidently [36].

The stability of 10%Co_3O_4/CeO_2-C catalyst was tested at 500 °C. The ethanol conversion was close to 100% and the product distribution was the same as listed in Table 1 of corresponding catalyst and reaction temperature. Decrease of the conversion, change of the H_2 yield and product distribution were not detected in the running period of 40 h.

Co/ZnO catalyst shows the best performance for SRE among cobalt-based catalysts reported [28]. It can keep 100% conversion and high H_2 selectivity for 50 h at 723 K with GHSV of 5000 h^{-1} and EtOH/H_2O/Ar of 1/13/70 (molar ratio). Over Co/ZnO catalyst, ethanol conversion cannot reach 100% when GHSV exceeds 15,000 h^{-1}. In particular, 10%Co_3O_4/CeO_2-C catalyst of this work showed comparable or even better catalytic performance for SRE. It should be noted that catalytic performance over 10%Co_3O_4/CeO_2-C was performed under much higher space velocity and lower water/ethanol ratio.

3.2. TG-DTA

Fig. 5 showed the thermal behavior of Co_3O_4/CeO_2 after the reaction with different preparation methods. For 10%Co_3O_4/CeO_2-I catalyst, two exothermic peaks appear between 200 and 500 °C, and it was in agreement with two steps of weight loss.

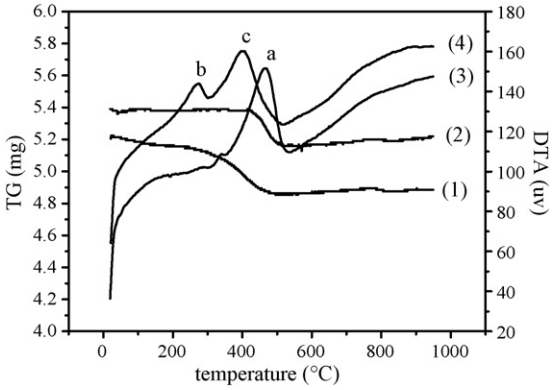

Fig. 5. TG-DTA curves of 10%Co_3O_4/CeO_2 catalysts after the reaction: (1) TG curve of 10%Co_3O_4/CeO_2-I; (2) TG curve of 10%Co_3O_4/CeO_2-C; (3) DTA curve of 10%Co_3O_4/CeO_2-C; (4) DTA curve of 10%Co_3O_4/CeO_2-I.

The weight loss for 10%Co_3O_4/CeO_2-C was 1.79% between 400 and 500 °C, and this corresponds to the exothermic peak at 467 °C, while the weight loss of 10%Co_3O_4/CeO_2-I was 6.37% including weight loss of two steps, indicating that the catalyst prepared by co-precipitation showed better carbon resistance.

From the TG-DTA results it could be seen that both the amount of carbon deposited and the carbon properties were different over catalysts prepared by different methods.

3.3. XRD

3.3.1. XRD results of Co_3O_4/CeO_2 catalysts prepared by different methods

Fig. 6 showed XRD patterns of Co_3O_4/CeO_2 catalysts prepared by different methods. Diffraction peaks of Co_3O_4 and CeO_2 could be observed [37]. The intensity of Co_3O_4 pattern

Table 2
Product distribution at 350, 400 and 450 °C over 10%Co_3O_4/CeO_2 catalysts[a]

Catalysts	Reaction temperature (°C)	C_2H_5OH conversion (%)	Product distribution S_i (%)					
			H_2	CO	CO_2	CH_4	Acetaldehyde	Acetone
10%Co_3O_4/CeO_2-C	350	39.1	68.1	5.6	11.1	0	9.1	6.1
10%Co_3O_4/CeO_2-C	400	54.1	69.0	6.2	13.5	0	5.2	6.1
10%Co_3O_4/CeO_2-C	450	82.1	69.6	5.0	14.5	0	4.7	6.2
10%Co_3O_4/CeO_2-I	350	12.6	64.0	0	4.1	0	16.8	15.1
10%Co_3O_4/CeO_2-I	400	15.7	65.4	0	5.6	0	10.9	18.1
10%Co_3O_4/CeO_2-I	450	18.8	65.1	4.1	6.4	0	8.8	15.6

[a] GHSV = 1,20,000 ml g_{cat}^{-1} h^{-1}

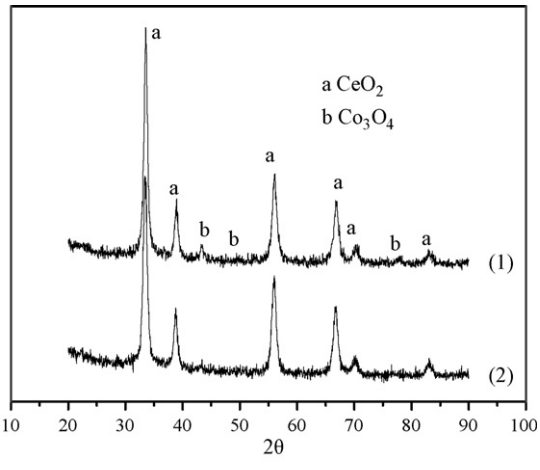

Fig. 6. XRD patterns of 10%Co_3O_4/CeO_2 catalysts prepared by different methods: (1) 10%Co_3O_4/CeO_2-C; (2) 10%Co_3O_4/CeO_2-I.

over 10%Co_3O_4/CeO_2-I catalyst was relatively weaker and broader, implying that Co_3O_4 was well dispersed on CeO_2 surface for catalyst prepared by impregnation method [38].

Table 3 showed the ceria lattice parameter calculated from ceria(1 1 1) reflection. The lattice parameters of ceria in Co_3O_4/CeO_2 catalysts become smaller, which should be ascribed to the incorporation of Co into the CeO_2 lattice. The detail will be discussed in Section 4.2 below.

3.3.2. *In situ XRD of 10%Co_3O_4/CeO_2-C*

Figs. 7 and 8 showed in situ XRD patterns of 10%Co_3O_4/CeO_2-C catalyst under reduction conditions. The XRD spectrum of unreduced sample exhibited diffraction patterns of CeO_2 and Co_3O_4. After reduction at 350 and 400 °C, a peak was observed at ($2\theta = 49.22$), which corresponds to the appearance of CoO(2 0 0). With the increase of reduction temperature from 450 to 600 °C, CoO(2 0 0) peak gradually disappeared while no diffraction peaks correspond to other cobalt species were observed. At 650 °C, diffraction peak ($2\theta = 51.53$) of metal cobalt(1 1 1) appeared and the intensity of Co(1 1 1) peak further increased with the increase of reduction temperature.

The reduction of Co_3O_4 was described as a two steps process ($Co_3O_4 \rightarrow CoO \rightarrow Co$) [39,40], although a single broad reduction profile is known in literatures. The data shown in Figs. 7 and 8 indicated that the Co_3O_4 reduction was in two steps: first, Co_3O_4 reduces to CoO at lower temperature, and then the CoO further reduced to metallic cobalt at higher temperature. The observed results are in line with the TPR results discussed in Section 3.4.

Meanwhile, the diffraction patterns of CeO_2 first became broader and then sharper, which should be due to that surface

Table 3
Lattice parameter and specific surface areas of Co_3O_4/CeO_2

Catalysts	Space distance between crystal face, d (Å)	CeO_2 lattice parameter, a (Å)	S_{BET} ($m^2\ g^{-1}$)
CeO_2	3.115	5.395	51.5
10%Co_3O_4/CeO_2-I	3.108	5.383	45.1
10%Co_3O_4/CeO_2-C	3.099	5.368	33.6

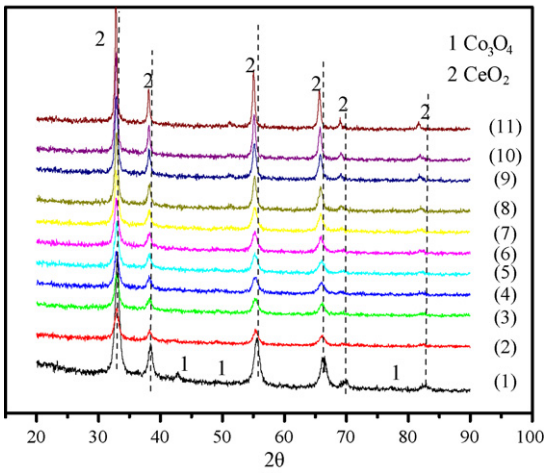

Fig. 7. In situ XRD of 10%Co_3O_4/CeO_2-C catalyst ($2\theta = 20$–$90°$): (1) fresh; reduction temperature: (2) 350 °C; (3) 400 °C; (4) 450 °C; (5) 500 °C; (6) 550 °C; (7) 600 °C; (8) 650 °C; (9) 700 °C; (10) 750 °C; (11) 800 °C, respectively.

CeO_2 was reduced at 350 °C (Figs. 8 and 9B) and ceria sintered at high reduction temperature respectively. The position of CeO_2 peaks was shifted towards lower 2θ degree in whole reduction process.

3.4. *TPR*

Fig. 9 showed TPR profiles of Co_3O_4/CeO_2 catalysts prepared by different methods. Table 4 listed the hydrogen consumption according to reduction peak areas and reduction temperature. As discussed above, cobalt oxide was reduced in two steps [41,42]. The TPR profile for pure Co_3O_4 showed two reduction peaks at 303 and 382 °C. The ratio of the reduction peak area of the second and the first step was 2.95, which was close to stoichiometric ratio of two-step reduction process. The low-temperature peak attributed to the reduction of Co_3O_4 to CoO and the second peak in the TPR curve was correspond to the reduction of CoO to the metallic cobalt.

As reported in the literatures, the reduction of ceria exhibits a low-temperature reduction peak at 437 °C and a

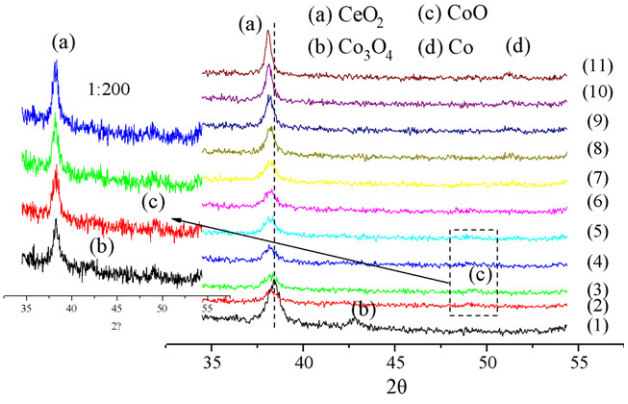

Fig. 8. In situ XRD of 10%Co_3O_4/CeO_2-C catalyst ($2\theta = 35$–$55°$): (1) fresh; reduction temperature: (2) 350 °C; (3) 400 °C; (4) 450 °C; (5) 500 °C; (6) 550 °C; (7) 600 °C; (8) 650 °C; (9) 700 °C; (10) 750 °C; (11) 800 °C, respectively.

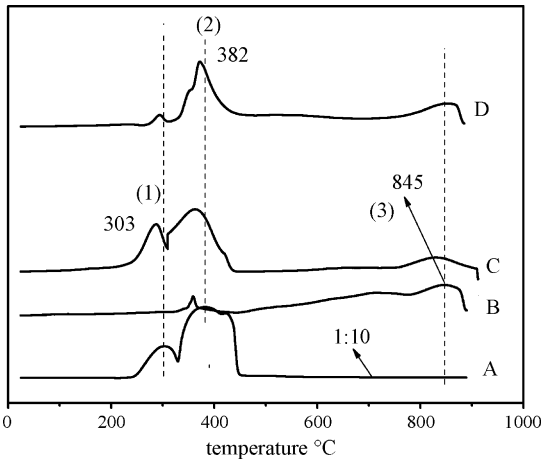

Fig. 9. H_2-TPR profiles of (A) Co_3O_4, (B) CeO_2, (C)10%Co_3O_4/CeO_2-C, (D) 10%Co_3O_4/CeO_2-I.

high-temperature peak at 825 °C. The two reduction temperatures are respectively attributed to the reduction of surface ceria and the reduction of bulk ceria [43,44]. In this work, two reduction peaks, one around 359 °C and the other close to 845 °C were observed on the pure CeO_2 sample. These two peaks are attributed to the reduction of surface and bulk CeO_2.

Three reduction peaks was seen in H_2-TPR curves of 10%Co_3O_4/CeO_2 catalysts with different preparation methods. Results of in situ XRD (Figs. 7 and 8) suggested that Co_3O_4 was reduced to CoO between 300 and 400 °C, and then reduced to metallic cobalt at 400 °C. Hence, the first reduction peaks can be ascribed to the reduction of Co_3O_4 to CoO. Because the area of second peak was much larger than the first one (the ratio was higher than two step reduction of pure Co_3O_4, see Table 4), the second peak should include both the reduction of cobalt incorporated ceria and the reduction of CoO to metal cobalt. Due to Co incorporation, the reduction of CeO_2 may become easier [45]. This point will be explained in discussion (see Section 4.2). In addition, we cannot eliminate the existence of CoO and other Co^{2+} in calcined samples.

4. Discussions

4.1. The synergy of Co_3O_4 and CeO_2 on catalytic performance

Relatively a lower ethanol conversion of below 60% was obtained over either pure Co_3O_4 or pure CeO_2 (Fig. 4) compared to a high ethanol conversion of close to 100% over the mixed Co_3O_4/CeO_2 catalysts, which clearly indicating the existence of a synergistic interaction between these two oxides. Ethanol dehydrogenation and dehydration were obvious over Co_3O_4 and CeO_2 catalysts. CeO_2 catalyst favors acetaldehyde condensation to acetone. Low ethanol conversion and high selectivity of C_2H_4 and aldehyde were observed over these two catalysts (Table 1). On the other hand, C_2H_4 was not detected over Co_3O_4/CeO_2 catalysts (Table 1). The formation of C_2H_4 readily leaded to coke formation.

4.2. The reduction behavior

The addition of CeO_2 influences the reduction of CoO_x, which can be ascribed to two reasons. On one hand, a high dispersion of CoO_x makes it easier to be reduced. From Fig. 9, both the reduction temperatures of C and D were lower than A. On the other hand, the chemical bond of Co–O–Ce on surface makes it difficult to be reduced for CoO_x. The dispersion of CoO_x in catalysts prepared by impregnation method was higher than catalysts prepared by co-precipitation method (Fig. 6). It results in more tendency to interact between CeO_2 and CoO_x on catalyst surface for catalysts prepared by impregnation. So from Fig. 9D and Table 4, it was seen that CoO_x was harder to be reduced when the catalyst was prepared by impregnation. Both the reduction temperature and hydrogen consumption indicated that Co_3O_4 in 10%Co_3O_4/CeO_2-C catalyst was more reducible. It is in agreement with higher activity of catalyst prepared by co-precipitation method than those made by impregnation method.

The second reduction peak (between 350 and 500 °C, Fig. 9C) observed in the TPR of 10%Co_3O_4/CeO_2-C included the reduction of bulk ceria and the reduction CoO. The increase of ceria lattice parameter in 10%Co_3O_4/CeO_2-C, as it was reduced at 350 °C and higher temperatures (Table 5), indicated formation of oxygen vacancies resulted from bulk reduction.

When CeO_2 was reduced at 350 °C, the intensity of its diffraction patterns became weaker than the unreduced catalyst, as shown in Figs. 7 and 10, and the lattice parameter moved towards larger value after reduction at 350 °C (Table 5).

The change of lattice parameter after the reduction at 750 °C indicated that more lattice oxygen in bulk is formed. That is corresponding to the reduction peak at 800 °C in H_2-TPR curve (Fig. 9C).

Comparing Co_3O_4/CeO_2 with pure CeO_2, CeO_2 lattice parameters in Co_3O_4/CeO_2 was much larger than that over

Table 4
H_2-TPR results of 10%Co_3O_4/CeO_2 catalysts prepared by different methods[a]

Sample (g)	Peak temperature (°C)			H_2 uptake (μmol/g)[a]		
	Peak (1)	Peak (2)	Peak (3)	Peak (1)	Peak (2)	Peak (3)
Co_3O_4 (0.032)	303	382	–	3442	10,152	–
10%Co_3O_4/CeO_2-C (0.030)	287	363	829	225	1,071	440
10%Co_3O_4/CeO_2-I (0.032)	294	372	848	98	487	315
CeO_2 (0.030)	–	359	845	–	84	1116

[a] Considering complete reduction of CuO as calculation standard.

Table 5
Lattice parameter of Co_3O_4/CeO_2 and CeO_2

Reduction temperature (°C)	Catalysts			
	10%Co_3O_4/CeO_2-C		CeO_2	
	Space distance between crystal face, d (Å)	CeO_2 lattice parameter, a (Å)	Space distance between crystal face, d (Å)	CeO_2 lattice parameter, a (Å)
Unreduced	3.099	5.368	3.115	5.395
350	3.148	5.452	3.123	5.409
400	3.148	5.452	3.123	5.409
450	3.156	5.466	3.123	5.409
500	3.156	5.466	3.131	5.423
550	3.156	5.466	3.131	5.423
600	3.156	5.466	3.131	5.423
650	3.156	5.466	3.131	5.423
700	3.156	5.466	3.131	5.423
750	3.164	5.480	3.131	5.423
800	3.164	5.480	3.131	5.423

CeO_2 (Table 5), when they were reduced. It showed the formation of more oxygen vacancies in ceria lattice of Co_3O_4/CeO_2 catalyst. It also indicated the incorporation of cobalt ions into the lattice of CeO_2.

As could be seen from the data in Table 3 for Co_3O_4/CeO_2 catalysts, the lattice parameter of CeO_2(1 1 1) decreased comparing with pure ceria, which should be due to the incorporation of cobalt ions into the CeO_2 lattice; and from Table 5, it was seen that lattice parameter of CeO_2(1 1 1) obviously increased with the increase of reduction temperature. The ceria lattice value over Co_3O_4/CeO_2 catalyst was much larger than pure CeO_2 at the same reduction temperature. When Co_3O_4/CeO_2 was unreduced, the incorporation of cobalt ions resulted in the contraction of ceria lattice, due to the smaller size of cobalt ions than that of the cerium ions. Here, the difference in electrical charge of Co(II or III) and Ce(IV) will cause electro-imbalance, which can be balanced by the surface adsorption. After reduction, this electro-neutrality is maintained in the solid by the formation of oxygen vacancies. Thus, the lattice parameter of CeO_2(1 1 1) becomes bigger.

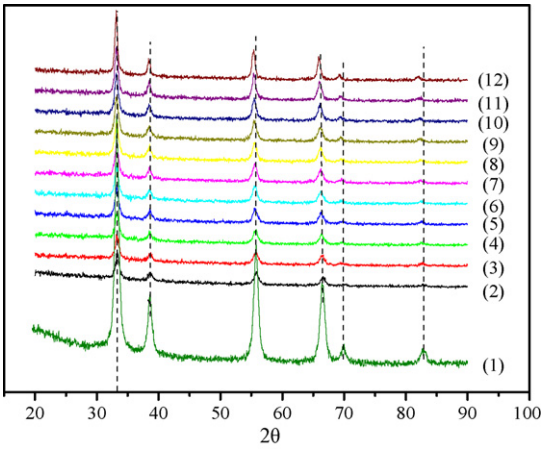

Fig. 10. In situ X-ray diffraction of pure CeO_2 ($2\theta = 20$–$90°$): (1) fresh; reduction temperature: (2) 350 °C; (3) 400 °C; (4) 450 °C; (5) 500 °C; (6) 550 °C; (7) 600 °C; (8) 650 °C; (9) 700 °C; (10) 750 °C; (11) 800 °C; (12) 850 °C, respectively.

4.3. The effect of preparation method on catalyst structure

Combined with all characterization results, the relationship between the structure of catalyst and catalytic performance was further discussed as follows. The BET surface area and the dispersion of Co_3O_4 were affected by preparation method. The catalyst prepared by impregnation method showed both higher BET surface area and higher dispersion of CoO_x. The Co_3O_4 was well dispersed on support for catalyst prepared by impregnation method, resulting in strong interaction between Co_3O_4 on catalyst surface and CeO_2. This was supported by H_2-TPR (Fig. 9) and XRD of Fig. 6. For 10%Co_3O_4/CeO_2-C catalyst, more cobalt ions incorporated into CeO_2 lattice, accompanying with weaker interaction on the surface. Thus, more Co_3O_4 was reduced, and more active component of cobalt was formed in Co_3O_4/CeO_2-C catalyst. That is the reason why catalyst prepared by co-precipitation method is more active than that of prepared by impregnation method (Table 2).

The replacement of some Ce^{4+} with smaller cobalt ions enhanced the oxygen storage of CeO_2. By comparison, more cobalt ions entered into the CeO_2 lattice for Co_3O_4/CeO_2-C catalyst, so it showed higher carbon-resistance capacity. That is proved by TG-DTA analysis (Fig. 5).

In summary, larger particle Co_3O_4 is easily reduced in Co_3O_4/CeO_2-C catalyst, while the strong interaction between Co_3O_4 and surface CeO_2 promotes the formation of Ce–O–Co in Co_3O_4/CeO_2-I catalyst. The Co_3O_4 is very difficult to be reduced because of this kind of chemical bond, so Co_3O_4/CeO_2-I catalyst shows a lower activity for SRE reaction (Table 2).

5. Conclusions

1. High ethanol conversion and hydrogen yield are obtained for SRE reaction over 10%Co_3O_4/CeO_2 catalyst made by co-precipitation and the catalyst exhibits good stability.
2. Co_3O_4/CeO_2 is much more active than either Co_3O_4 or CeO_2 indicating the existence of a synergistic effect between Co_3O_4 and CeO_2.

3. In situ XRD and TPR studies indicate that the reduction of CoO_x is influenced by its interaction with CeO_2.
4. The catalyst preparation method influences the interaction between cobalt and CeO_2. In comparison with catalysts prepared by impregnation, more cobalt ions enter into CeO_2 lattice when the catalyst is prepared by co-precipitation method, which results in weaker interaction between active phase and ceria on surface of Co_3O_4/CeO_2. Thus, the cobalt oxides in co-precipitated catalysts are more reducible and metal cobalt reduced from them is the key active component, hence the co-precipitated catalysts are more active. Meanwhile, more cobalt ions can be incorporated into ceria lattice and the incorporation of cobalt ions into CeO_2 crystal lattice is beneficial for resistance to carbon deposition.

Acknowledgements

The financial support of this work by Hi-tech Research and Development Program of China (863 program, Granted as No. 2006AA05Z115) and by Program for Changjiang Scholars and Innovative Research Team in University are gratefully acknowledged.

References

[1] Y. Tanaka, T. Utaka, R. Kikuchi, K. Sasaki, K. Eguchi, Appl. Catal. A 242 (2003) 287.
[2] S. Velu, K. Suzuki, T. Osaki, Catal. Lett. 69 (2000) 43.
[3] R. Craciun, W. Daniell, H. Knözinger, Appl. Catal. A 230 (2002) 153.
[4] V.V. Galvita, G.L. Semin, V.D. Belyaev, V.A. Semikolenov, P. Tsiakaras, V.A. Sobyanin, Appl. Catal. A 220 (2001) 123.
[5] M. Momirlan, T. Veziroglu, Renew. Sustainable Energy Rev. 3 (1999) 219.
[6] D. Das, T. Veziroglu, Int. J. Hydrogen Energy 26 (2001) 13.
[7] A.N. Fatsikostas, D.I. Kondarides, X.E. Verykios, Catal. Today 75 (2002) 145.
[8] A. Haryanto, S. Fernando, N. Murali, S. Adhikari, Energy Fuels 19 (2005) 2098.
[9] J. Llorca, P.R. Piscina, J. Sales, N. Homs, Chem. Commun. 7 (2001) 641.
[10] J.P. Breen, R. Burch, H.M. Coleman, Appl. Catal. B 39 (2002) 65.
[11] S. Cavallaro, V. Chiodo, V. Vita, S. Freni, J. Power Sources 123 (2003) 10.
[12] C. Diagne, H. Idriss, A. Kiennemann, Catal. Commun. 3 (2002) 565.
[13] R.M. Navarro, M.C.A. Ívarez-Galvań, M.C. Sańchez-Sańchez, F. Rosa, J.L.G. Fierro, Appl. Catal. B 55 (2005) 229.
[14] D.K. Liguras, D.I. Kondarides, X.E. Verykios, Appl. Catal. B 43 (2003) 345.
[15] S. Cavallaro, V. Chiodo, S. Freni, N. Mondello, F. Frusteri, Appl. Catal. A 249 (2003) 119.
[16] S. Freni, S. Cavallaro, N. Mondello, L. Spadaro, F. Frusteri, J. Power Sources 108 (2002) 53.
[17] D. Srinivas, C.V.V. Satyanarayana, H.S. Potdar, P. Ratnasamy, Appl. Catal. A 246 (2003) 323.
[18] F. Mariño, M. Boveri, G. Baronetti, M. aborde, Int. J. Hydrogen Energy 26 (2001) 665.
[19] F. Frusteri, S. Freni, V. Chiodo, L. Spadaro, G. Bonura, S. Cavallaro, J. Power Sources 132 (2004) 139.
[20] C. José, M. Fernando, L. Miguel, A. Norma, Chem. Eng. J. 98 (2004) 61.
[21] S. Cavallaro, S. Freni, Int. J. Hydrogen Energy 21 (1996) 465.
[22] S. Velu, N. Satoh, C.S. Gopinath, K. Suzuli, Catal. Lett. 82 (2002) 145.
[23] M.S. Batista, R.K.S. Santos, E.M. Assaf, J.M. Assaf, E.A. Ticianelli, J. Power Sources 124 (2003) 99.
[24] K. Urasaki, K. Tokunaga, Y. Sekine, E. Kikuchi, M. Matsukata, Chem. Lett. 34 (2005) 668.
[25] M.S. Batista, R.K.S. Santos, E.M. Assaf, J.M. Assaf, E.A. Ticianelli, J. Power Sources 134 (2004) 27.
[26] J. Llorca, N. Homs, P.R. Piscina, J. Catal. 227 (2004) 556.
[27] J. Llorca, N. Homs, J. Sales, J.G. Fierro, P.R. Piscina, J. Catal. 222 (2004) 470.
[28] J. Llorca, N. Homs, J. Sales, P.R. Piscina1, J. Catal. 209 (2002) 306.
[29] S. Cavallaro, N. Mondello, S. Freni, J. Power Sources 102 (2001) 198.
[30] J. Llorca, J. Dalmon, P.R. Piscina, N. Homs, Appl. Catal. A 243 (2003) 261.
[31] R.J. Gorte, S. Zhao, Catal. Today 104 (2005) 18.
[32] J. Kugai, S. Velu, C.S. Song, Catal. Lett. 101 (2005) 255.
[33] J. Kugai, S. Velu, C.S. Song, M.H. Engelhard, Y.H. Chin, J. Catal. 238 (2006) 430.
[34] M. Kraum, M. Baerns, Appl. Catal. A 186 (1999) 189.
[35] M. Kang, M.W. Song, C.H. Lee, Appl. Catal. A 251 (2003) 143.
[36] J. Llorca, P. Piscina, J.-A. Dalmon, J. Sales, N. Homs, Appl. Catal. B 43 (2003) 355.
[37] B. Ernst, L. Hilaire, A. Kiennemann, Catal. Today 50 (1999) 413.
[38] L. Spadaro, F. Arena, M.L. Granadosc, M. Ojedac, J.L.G. Fierro, F. Frusteri, J. Catal. 234 (2005) 451.
[39] H.F.J. van't Blik, R. Prins, J. Catal. 97 (1986) 188.
[40] B. Sexton, A. Hughes, T. Turney, J. Catal. 97 (1986) 390.
[41] G. Jacobs, T.K. Das, Y. Zhang, J.L. Li, G. Racoillet, B.H. Davis, Appl. Catal. A 233 (2002) 263.
[42] B. Viswanathan, R. Gopalakrishnan, J. Catal. 99 (1986) 342.
[43] D. Terribile, A. Trovarelli, C. Leitenburg, A. Primavera, G. Dolcetti, Catal. Today 47 (1999) 133.
[44] J. Kaspar, P. Fornasiero, M. Graziani, Catal. Today 50 (1999) 285.
[45] L.F. Liotta, G. Di Carlo, G. Pantaleo, G. Deganello, Catal. Commun. 6 (2005) 329.